

## Article

# High-Performance and Low-Cost Membranes Based on Poly(vinylpyrrolidone) and Cardo-Poly(etherketone) Blends for Vanadium Redox Flow Battery Applications

Tong Mu, Shifan Leng, Weiqin Tang, Ning Shi, Guorui Wang and Jingshuai Yang \*

Department of Chemistry, College of Sciences, Northeastern University, Shenyang 110819, China

\* Correspondence: yjs@mail.neu.edu.cn

**Abstract:** Energy storage systems have aroused public interest because of the blooming development of intermittent renewable energy sources. Vanadium redox flow batteries (VRFBs) are the typical candidates owing to their flexible operation and good cycle durability. However, due to the usage of perfluorinated separator membranes, VRFBs suffer from both high cost and serious vanadium ions cross penetration. Herein, we fabricate a series of low-budget and high-performance blend membranes from polyvinylpyrrolidone (PVP) and cardo-poly(etherketone) (PEKC) for VFRB. A PEKC network gives the membrane excellent mechanical rigidity, while PVP endows the blend membranes with superior sulfonic acid uptake owing to the present N-heterocycle and carbonyl group in PVP, resulting in low area resistance. Meanwhile, blend membranes also display low vanadium ion permeability resulting from the electrostatic repulsion effect of protonated PVP polymer chains towards vanadium ions. Consequently, the 50%PVP-PEKC membrane has a high ionic selectivity of  $1.03 \times 10^6 \text{ S min cm}^{-3}$ , while that of Nafion 115 is nearly 17 times lower ( $6.03 \times 10^4 \text{ S min cm}^{-3}$ ). The VRFB equipped with 50%PVP-PEKC membrane has high coulombic efficiencies (99.3–99.7%), voltage efficiencies (84.6–67.0%) and energy efficiencies (83.9–66.8%) at current densities of  $80\text{--}180 \text{ mA cm}^{-2}$ , and possesses excellent cycle constancy, indicating that low-cost x%PVP-PEKC blend membranes have a great application potentiality for VRFBs.

**Keywords:** blend membrane; poly(vinylpyrrolidone); cardo-poly(etherketone); vanadium redox flow battery; low cost



**Citation:** Mu, T.; Leng, S.; Tang, W.; Shi, N.; Wang, G.; Yang, J. High-Performance and Low-Cost Membranes Based on Poly(vinylpyrrolidone) and Cardo-Poly(etherketone) Blends for Vanadium Redox Flow Battery Applications. *Batteries* **2022**, *8*, 230. <https://doi.org/10.3390/batteries8110230>

Academic Editor: Catia Arbizzani

Received: 4 October 2022

Accepted: 7 November 2022

Published: 10 November 2022

**Publisher's Note:** MDPI stays neutral with regard to jurisdictional claims in published maps and institutional affiliations.



**Copyright:** © 2022 by the authors. Licensee MDPI, Basel, Switzerland. This article is an open access article distributed under the terms and conditions of the Creative Commons Attribution (CC BY) license (<https://creativecommons.org/licenses/by/4.0/>).

## 1. Introduction

Energy shortage and environmental pollution have always been important issues of concern to modern society. Severe environmental problems and increasing consumption of fossil fuels have forced people to seek environmentally friendly renewable energies, such as wind and solar energy. However, an important problem faced by the application of these new energy sources in real life is the instable output [1]. It is urgent to combine these renewable energy sources with energy storage to achieve stable output. The vanadium redox flow battery (VRFB) is considered as the potential massive-scale energy storage device, which receives extensive attentions because of its flexible operation, high efficiency, long life and low manufacturing cost [2–5]. As an integral part of VRFB, the separator membrane is in charge of ionic conduction and preventing cross-mingling of redox-active substances. Thus, the membranes in VRFB need to possess good ion conductivity, low vanadium ion penetration, excellent chemical resistance, good mechanical integrity, and low commercial cost [6–8].

Thus far, the Nafion series membranes from DuPont are the most typically commercial membranes resulting from its high proton conductivity and mechanical properties [5,9–11]. However, their severe cross-penetration of vanadium ions and high manufacturing cost restrict the extensive application in VRFBs [2,6,10]. In recent years, researchers sought

materials that can replace Nafion for VRFBs, such as low-priced non-fluoroaromatic sulfonated poly (ether ether ketone) (SPEEK) [4,12]. However, SPEEK-based membranes still faced with significant crossover of vanadium ions, because that SPEEK has an inherent affinity for cations species, which promotes the migration of vanadium ions along with protons [13,14]. Moreover, the SPEEK membrane still confronts the challenge of its chemical stability, since the protonated aryl ether bonds are easy to cleave because of the attack of vanadium oxygen species, particularly the existence of the strong electron-withdrawing sulfonic acid groups [12,15,16].

Since the electrolytes used in VRFBs are based on a sulfuric acid (SA) solution, non-ionic membranes that do not conduct ions themselves can be selected as the separator for VRFBs. The polybenzimidazole (PBI) membrane is a representative, which can be doped with acid to achieve ion conduction [17,18]. Simultaneously, the SA-doped PBI membrane exhibits quite low vanadium ion permeability resulting from the electrostatic repulsion between vanadium species and the positively charged protonated polymer chain [19,20]. Zhao et al. firstly used sulfuric acid-absorbing PBI membrane for VRFBs, but its energy efficiency was extremely low because of the higher area resistance [18]. From the perspective of ions conducting mechanism, the acid absorbing content of sulfuric acid doped PBI membranes has a significant effect on the ionic conductivity. Therefore, many modifications have been done to upgrade the sulfuric acid uptake and reduce the area resistance of PBI membranes, including grafting bulky side-chain groups [21,22] and preparation of porous PBI membranes [23,24]. Nevertheless, the PBI polymer usually suffers from poor solubility in normal organic solvents and the use of carcinogenic 3,3',4,4'-tetraaminobiphenyl monomer during the polymer synthesis progress, which would limit its large-scale application [25].

Polyvinylpyrrolidone (PVP) is a commercial and low-cost industrial polymer, which has been widely used in various research fields, such as the lithium battery [26], water electrolysis [27], antibacterial materials [28], gene carriers [29], food additives [30], surfactants [31] and coatings [32]. Owing to the presence of N-heterocyclic rings and carbonyl groups, PVP has an excellent acid absorption capability via acid-base interaction and hydrogen bonding [33,34]. However, pure PVP membrane is highly hydrophilic and even dissolves in water at room temperature, resulting to poor mechanical stability. Therefore, blending PVP with other enhanced materials are normally adopted in order to prepare mechanically tough membranes. For example, Lu et al. used this concept to prepare polyvinylidene fluoride blended PVP membranes, which exhibited superior phosphoric acid absorption capability and were employed as high temperature proton exchange membranes for fuel cells [35]. In our previous work, we fabricated five different PVP blended membranes using five kinds of engineering thermoplastics [34]. Results indicate that blending aromatic polymers can largely enhance the mechanical integrity of PVP blend membranes comparing with blending aliphatic polymers. Recently, several reinforced PVP blend membranes have been successively employed as separator membranes for VRFBs [33,36–38]. For example, Lu and co-workers fabricated highly ion-selective membranes by blending PVP and poly (ether sulfone), which displayed high coulombic efficiency (98%) and excellent stability within 2000 h long-term cycling tests [33]. However, it is worth noting that a higher content of PVP brings lower area resistance (AR) accompanied by more severe vanadium ion penetration. Therefore, the balance between proton migration and vanadium ion penetration of non-ionic membranes in VRFB is still a challenge.

In this paper, we extend our previous work [34,38] to employ PVP and cardo-poly(etherketone) (PEKC) blend membranes to be used as the separator in VRFBs. Due to the existence of amide groups in the backbone, PVP is highly polar and has a good solubility in most strongly polar solvents [39]. PEKC was chosen as the enhanced material due to following advantages including low cost, excellent mechanical and chemical toughness [40,41]. Meanwhile the existence of cardo group is contributed to the dissolution of PEKC in organic solvents [42]. Our previous works found that PEKC exhibited good compatibil-

ity with poly(ethylene imine) [40], 1-(3-aminopropyl) imidazole functionalized polyvinyl chloride [41] and Tröger's base polymer [43]. In addition, the Flory–Huggins interaction parameter can also be used to explain the thermodynamic compatibility of polymers [39,44]. Herein, adopting a straightforward solution casting procedure, various PVP-PEKC blend membranes have been fabricated for VRFBs. The obtained blend membranes brought in the benefit of the two components, such as the superior SA uptake, improved dimensional stability, reduced vanadium ion penetration, decreased area resistance and high mechanical integrity. Performance and cycling life of the single VRFB were determined to evaluate the technical feasibility of the  $x\%$ PVP-PEKC blend membranes for VRFB applications.

## 2. Experimental Section

### 2.1. Materials

Polyvinylpyrrolidone (PVP, average M.W. 1,300,000) and cardo-poly(etherketone) (PEKC) (inherent viscosity: 0.78 dL g<sup>-1</sup>) were provided by J&K Scientific (Beijing, China) and Jida High Performance Materials Co., Ltd. (Changchun, China), respectively. Vanadyl sulfate hydrate ( $\text{VOSO}_4 \cdot 3\text{H}_2\text{O}$ ) was purchased from Haizhongtian Chemical Company (Shenyang, China). Magnesium sulfate (anhydrous,  $\text{MgSO}_4$ ), N, N-Dimethylacetamide (DMAc) and other chemicals were purchased from Sinopharm Chemical Reagent Co., Ltd. (Shanghai, China). All the chemical reagents and polymers used in this work have not undergone any pre-treatment.

### 2.2. Fabrication of PVP-PEKC Membranes

PVP and PEKC were separately dissolved in DMAc to receive PVP/DMAc and PEKC/DMAc solutions with the same concentration of 5 wt%. Then, two solutions were mixed in the light of a certain mass ratio of PVP to PEKC. After stirring at room temperature (RT) for 24 h, the uniform and transparent solution was subsequently poured onto the Petri dish and dried at 80 °C for 12 h. The Petri dish taken out of the oven was immersed in water to strip membrane, which was washed using deionized water to remove DMAc, finally dried at 100 °C for 8 h. The consequent blend membranes were recorded as  $x\%$ PVP-PEKC, and  $x\%$  (i.e.,  $x = 25, 35, 50, 60$  and  $75$ ) represented the adding mass ratio of PVP to PEKC. The fabrication procedure of blend membranes is illustrated in Figure 1.

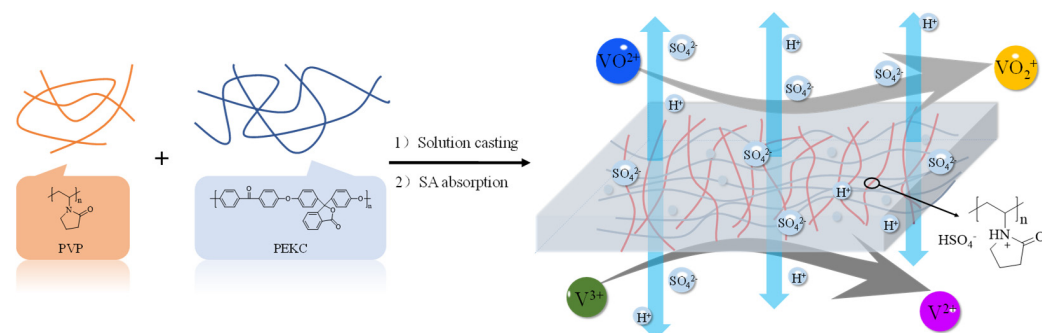


**Figure 1.** The schematic of fabricating  $x\%$ PVP-PEKC blend membranes.

### 2.3. Characterization

The characterizations in terms of Fourier transform infrared (FT-IR) spectrum, scanning electron microscope (SEM), water uptake (WU%), acid doping content (ADC%), acid doping level (ADL), dimensional swellings, mechanical properties, area resistance (AR), permeability of vanadium ion and the chemical stability of membranes were determined, the methods of which were presented in the supporting information. The ADC% is defined as the SA mass percent per gram of the membrane, while ADL of one membrane is defined as the number of SA molecules per PVP repeat unit.

#### 2.4. VRFB Test

The VRFB was assembled and tested based on our previous work [24]. The effective area of electrodes was  $9\text{ cm}^2$  ( $3 \times 3\text{ cm}$ ), while both positive and negative electrodes employed 25 mL of 1.65 M  $\text{V}^{3+}/\text{VO}^{2+}$  in 3.0 M  $\text{H}_2\text{SO}_4$  as the cell electrolyte. The details are described in the supporting information. According to Equations (1)–(3), the coulombic efficiency ( $CE$ ), energy efficiency ( $EE$ ) and voltage efficiency ( $VE$ ) are calculated.

$$CE(\%) = \frac{\int I_d dt}{\int I_c dt} \times 100\% \quad (1)$$

$$EE(\%) = \frac{\int V_d I_d dt}{\int V_c I_c dt} \times 100\% \quad (2)$$

$$VE(\%) = \frac{EE}{CE} \times 100\% \quad (3)$$

where  $I$  and  $V$  mean the current and voltage;  $t$  is the time; and  $d$  and  $c$  present the discharge and charge processes.

### 3. Results and Discussion

#### 3.1. Fabrication of Membranes

PVP is a significantly hydrophilic polymer, while PEKC is a chemically inert engineering thermoplastic with high mechanical strength and excellent solubility in organic solvents. During the solution-casting progress, different PVP and PEKC macromolecular chains move and become entangled with each other, forming a homogeneous phase in DMAc. Through the straightforward solution-casting method, the  $x\%$ PVP-PEKC blend membranes were prepared. The optical and SEM images of 25%PVP-PEKC, 50%PVP-PEKC and 75%PVP-PEKC membranes are depicted in Figures 2A and S1. As seen in Figure 2A, all the prepared blend membranes are uniform, transparent and flexible. Moreover, membranes become more and more wrinkled as the content of PVP in membranes increased, probably due to the high hydrophilicity of PVP. Figure S1 shows that the three blend membranes are non-porous and dense, indicating no phase separation between PVP and PEKC [15,38].



**Figure 2.** Digital images (A) of 25%PVP-PEKC (1), 50%PVP-PEKC (2) and 75%PVP-PEKC (3).

#### 3.2. FT-IR

FT-IR is used to determine the chemical structure of blend membranes as depicted in Figure 3. As to PEKC, the lactone group ( $\text{O}-\text{C}=\text{O}$ ) and aryl ether band ( $\text{C}-\text{O}-\text{C}$ ) display absorption bands at  $1771\text{ cm}^{-1}$  and  $1235\text{ cm}^{-1}$ , respectively [45]. For PVP, the characteristic peaks at  $2957\text{--}2866\text{ cm}^{-1}$ ,  $1657\text{ cm}^{-1}$ , and  $1284\text{ cm}^{-1}$  can be appointed as the stretching vibration of  $-\text{CH}_2-$ , carbonyl group and C-N bond, respectively [34,35]. Meanwhile, these characteristic peaks also appear in FT-IR spectra of  $x\%$ PVP-PEKC membranes, while the strength of abovementioned peaks increase as increasing the PVP content of  $x\%$ PVP-PEKC membranes. FT-IR spectra confirm that the PVP has been successfully blended in PEKC.

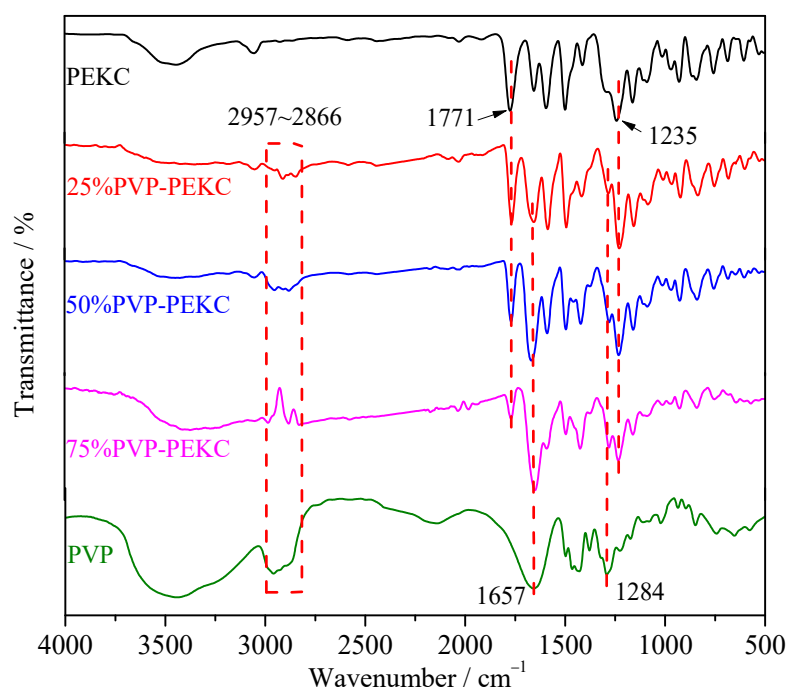


**Figure 3.** FT-IR spectra of PEKC, PVP and various blended x%PVP-PEKC membranes.

### 3.3. Water Uptake, Acid Doping Content and Acid Doping Level

Previous studies of the ionic transport of acid absorbed membranes have confirmed the importance of their water content and acid uptake [22,46]. Thus, all the x%PVP-PEKC membranes were submersed in 3 M H<sub>2</sub>SO<sub>4</sub> solution to achieve the ionic conduction of blend membranes. Owing to the strong interactions of N-heterocycle and carbonyl groups in PVP with SA molecules, the x%PVP-PEKC blend membranes possessed excellent SA absorption capability, and were also equipped with good dimensional and mechanical properties [34]. Figure 4A shows both the WU% and ADC% of x%PVP-PEKC blend membranes upgraded as the increase in the PVP content of membranes. Consequently, the 75%PVP-PEKC membrane achieved the highest WU% and ADC% of 45.2% and 33.3% after submerging in 3 M H<sub>2</sub>SO<sub>4</sub> at RT. The results show that the introduction of PVP enhanced the hydrophilicity of the blend membranes and improved the water/SA absorption capacity, which would increase the ion conductivity of the blend membranes.

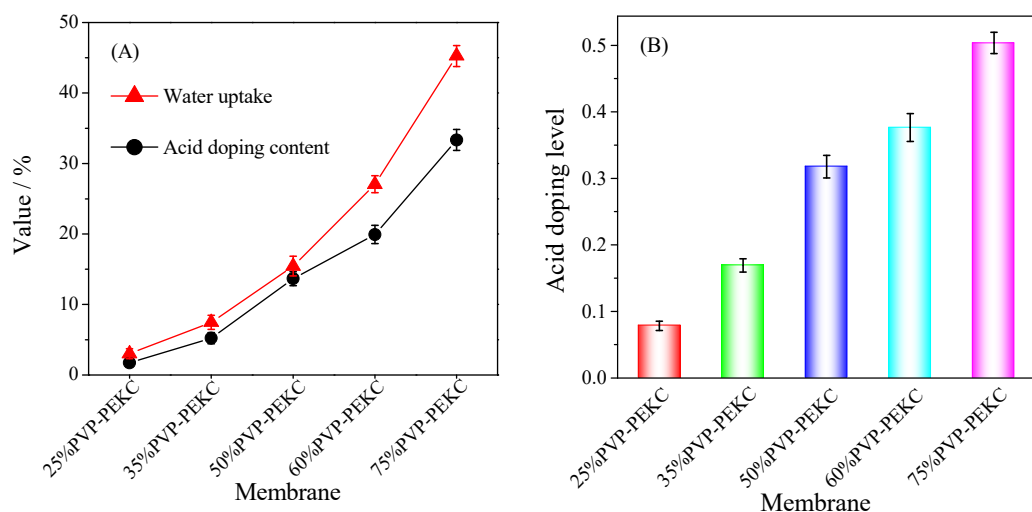


**Figure 4.** Water uptake, acid doping content (A), and acid doping level (B) of various blend membranes after submerging in 3 M H<sub>2</sub>SO<sub>4</sub> solution at RT.

In order to detect the interaction of SA molecules with blend membranes, the ADLs of blend membranes have been calculated. Figure 4B shows ADL results of  $x\%$ PVP-PEKC blend membranes. Obviously, the ADL of the blend membranes enhanced with the increased PVP content in agreement with the ADC% trend. Nonetheless, the ADLs of all blend membranes were below 1, indicating that the SA molecules protonated the PVP through the acid-base interaction, which were in the form of “bound acid” in the blend membranes rather than “free acid” [19,22]. This would have a big influence on the ion transport, which will be discussed in the Section 3.5.

### 3.4. Swelling and Mechanical Properties

The high ADC% of the membrane would be beneficial to reduce the AR, but would bring about dreadful swelling. Figure 5 shows that the volume swelling upgraded greatly with the increase of the PVP content, which is positively associated with the ADC% results. As an example, the volume swellings of 60%PVP-PEKC and 75%PVP-PEKC membranes were as high as 118% and 192%. This indicates that the volume swelling of the blend membrane is closely related and proportional to its acid absorption content, which has been commonly reported for phosphoric acid-doped membranes [19,34]. Thus, it is crucial that a suitable PVP content for blend membranes should be chosen for preparing the membrane with high SA absorption content and low swelling concurrently.

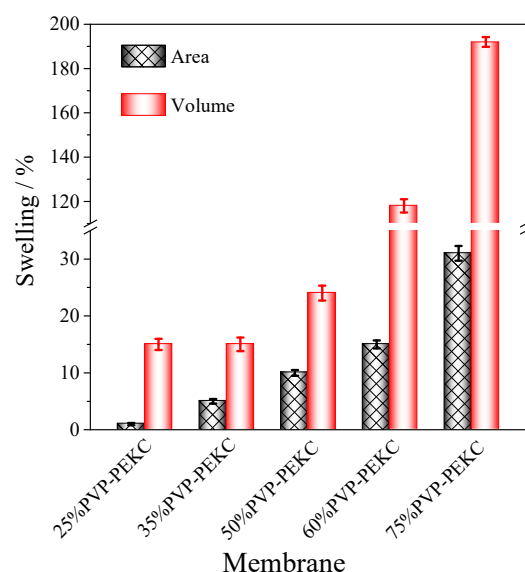


**Figure 5.** Dimensional swellings of various  $x\%$ PVP-PEKC blend membranes at RT.

For long-term operation of VRFBs, the mechanical properties of the membrane are particularly important [22]. Figure 6 presents the tensile stress–strain curves of  $x\%$ PVP-PEKC blend membranes after doping in 3M H<sub>2</sub>SO<sub>4</sub> at RT. The mechanical strength of membranes is opposite to the content of PVP in  $x\%$ PVP-PEKC blend membranes, which is consistent with our previous work on PVP and PBI blend membranes [38]. For instance, when the mass ratio of PVP to PEKC raised from 25% to 75%, the ADC% increased from 1.7% to 33.3% and the mechanical strength of blend membranes declined from 72 MPa to 16 MPa. This is mainly because the more PVP content, the more SA molecules doped into the blend membranes. The ADC% values of 25%PVP-PEKC and 75%PVP-PEKC membranes were 1.7% and 33.3%, respectively. Thus, the absorbed SA molecules brought in a serious plasticization effect, resulting in decreased mechanical strength. This phenomenon has also been widely reported for phosphoric acid doped membranes [19,42,47]. Meanwhile, all the membranes except 75%PVP-PEKC displayed similar elongation values of around 10%. However, the 75%PVP-PEKC membrane exhibited a significantly high elongation of 68%,

mainly due to its high acid uptake. The above results indicate that blending PEKC would largely enhance the tensile strength of membranes.

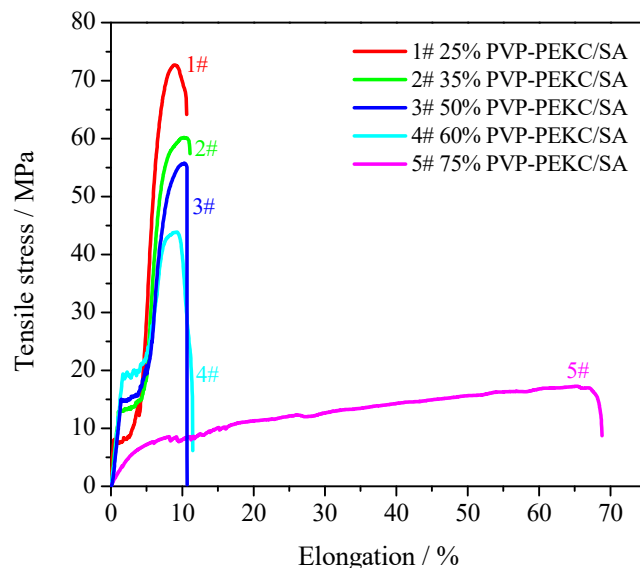


**Figure 6.** Tensile properties of various x%PVP-PEKC blend membranes at RT.

### 3.5. Area Resistance, Vanadium Ion Permeability and Ion Selectivity

Generally speaking, VRFBs obtaining high energy efficiency must equip with membranes of extremely low AR [2,10]. It is widely shared that the AR of one SA doped membrane is closely related to its acid uptake [17,19] and thickness [10,48]. The thickness of all x%PVP-PEKC blend membranes after doped with sulfuric acid is about 40  $\mu\text{m}$  in the present work. Figure 7A shows that the AR of x%PVP-PEKC membranes decreased as the increased PVP content of membranes, evidently owing to the increased SA uptake. As a result, the ARs of 50%PVP-PEKC, 60%PVP-PEKC and 75%PVP-PEKC membranes were less than  $0.31 \Omega \text{ cm}^2$ , which were comparable to Nafion212 ( $0.26 \Omega \text{ cm}^2$ ) and lower than that of Nafion115 ( $0.62 \Omega \text{ cm}^2$ ), while those of 25%PVP-PEKC and 35%PVP-PEKC membranes were as high as  $439.91 \Omega \text{ cm}^2$  and  $12.28 \Omega \text{ cm}^2$ , respectively. The analysis of AR results proves that the existence of PVP is important to enhance the acid absorption and reduce the AR. It should be noted that the precise ion transport mechanism in x%PVP-PEKC membranes is unclear. As discussed in Section 3.3, since all the SA molecules interacted with PVP via acid-base interaction, the sulfate ions attached to protonated PVP should be in charge of the internal circuit current. However, membranes are saturated with the liquid SA electrolyte, and the proton mobility ( $36.3 \times 10^{-8} \text{ m}^2 \text{ V}^{-1} \text{ s}^{-1}$ ) is rather higher than that of sulfate ions ( $8.3 \times 10^{-8} \text{ m}^2 \text{ V}^{-1} \text{ s}^{-1}$ ) [49]. Thus, we presume that protons also contributed to the conductivity of membranes, as depicted in Figure 1. Additionally, the ionic conductivity of each membrane can be calculated by dividing the thickness of the membrane by AR [50]. As a result, the ionic conductivities of 25%PVP-PEKC and 35%PVP-PEKC were much lower than  $1 \text{ mS cm}^{-1}$ , while those of 50%PVP-PEKC, 60%PVP-PEKC and 75%PVP-PEKC membranes were as high as  $11.3$ ,  $18.6$  and  $42.0 \text{ mS cm}^{-1}$ , respectively. Ionic conductivity results further confirmed that the existence of PVP is beneficial to the ion conduction.

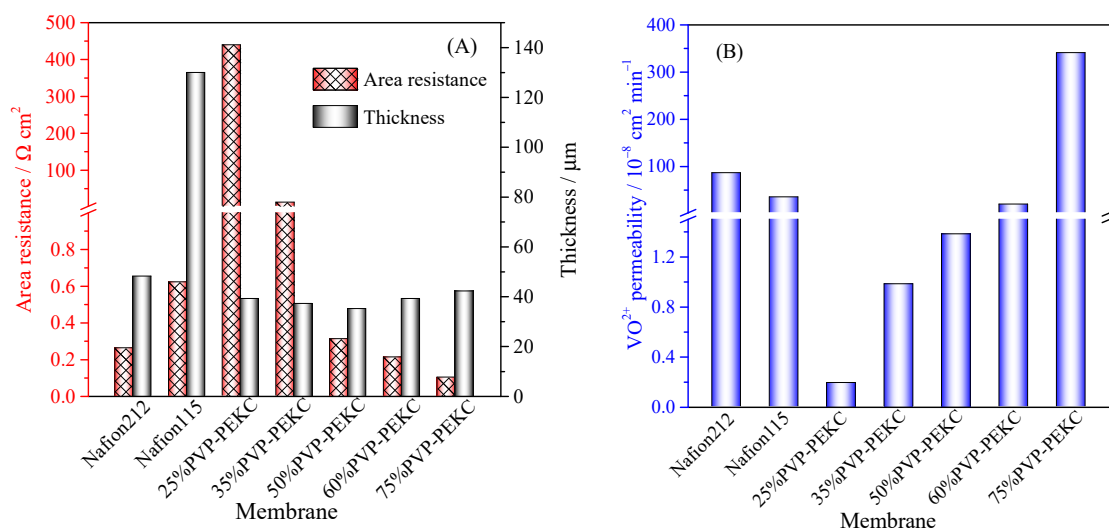


**Figure 7.** (A) Area resistance and thickness and (B) vanadium ion permeability of various membranes after immersing in 3 M  $\text{H}_2\text{SO}_4$  at RT.

Another vital parameter of one membrane is the vanadium ion permeability [2,6], which leads to self-discharge (capacity decay) and a decline in CE of the battery [51]. Figure 7B shows the vanadium ion permeability of various x%PVP-PEKC membranes. Apparently, the vanadium ion permeability elevated as the increased content of PVP in blend membranes. The vanadium ion permeability of 25%PVP-PEKC, 35%PVP-PEKC and 50%PVP-PEKC membranes (i.e.,  $1.9 \times 10^{-9} \text{ cm}^2 \text{ min}^{-1}$ ,  $9.8 \times 10^{-9} \text{ cm}^2 \text{ min}^{-1}$  and  $1.38 \times 10^{-8} \text{ cm}^2 \text{ min}^{-1}$ , respectively) was much lower than that of Nafion212 ( $8.61 \times 10^{-7} \text{ cm}^2 \text{ min}^{-1}$ ) and Nafion115 ( $3.48 \times 10^{-7} \text{ cm}^2 \text{ min}^{-1}$ ). The excellent resistance to vanadium ions of those membranes could be attributed to their low volume swellings. Meanwhile, the electrostatic repulsion between the protonated PVP macromolecular chains and  $\text{VO}_2^+$  ions was another clue to the low vanadium ion permeability [6,33,52]. It is worth noting that the vanadium ion permeability of 60%PVP-PEKC and 75%PVP-PEKC membranes was comparable to or nearly 10 times higher than that of Nafion115. The above results disclose that the abundant PVP contributed to significant SA uptake and deformation, resulting in largely increased vanadium ion permeability.

In order to comprehensively consider the impact of AR and vanadium (IV) ion permeability, the ion selectivity is evaluated by dividing the ionic conductivity by the vanadium ion permeability [21,24,53]. A superior selectivity value is indicative that the membrane is more likely to promote the transfer of charged carrying ions rather than the  $\text{VO}_2^+$  ions. As shown from Figure 8, the 50%PVP-PEKC membrane exhibited the highest ion selectivity of  $103 \times 10^4 \text{ S min cm}^{-3}$ , which is nearly 38 and 17 times higher than that of Nafion212 (i.e.,  $2.70 \times 10^4 \text{ S min cm}^{-3}$ ) and Nafion115 (i.e.,  $6.03 \times 10^4 \text{ S min cm}^{-3}$ ). Thus, the 50%PVP-PEKC membrane was more advantageous in the application of VRFBs owing to its higher ion selectivity.

### 3.6. Chemical Stability

The chemical stability of various x%PVP-PEKC membranes were determined by immersing membrane samples in the 1.5 M  $\text{VO}_2^+$  and 3 M  $\text{H}_2\text{SO}_4$  solution at RT for 350 h. As shown in Figure 9, after immersing for 350 h, all the membranes maintained their intact shape, while the weight retention ratio was higher than 97%. In addition, the 25%PVP-PEKC membrane with the lowest PVP percentage almost retained its transparency, while the color of other membranes with higher PVP contents became brown or dark green. As previously reported, the color of membranes became darker after chemical stability test, which might be attributed to the absorption of vanadium ions [54]. As seen from Figure 4A, the different PVP-PEKC blend membranes displayed different hydrophilicity, and both water uptake and acid doping content increased as the increase of the PVP content. As

a result, the vanadium ions might tend to be absorbed in the blend membrane with a high PVP percentage, so the color of the membranes with higher PVP contents darkened. Nevertheless, more investigations should be done to understand this phenomenon clearly. The chemical stability test results indicate that  $x\%$ PVP-PEKC membranes exhibited the superior chemical stability in the harsh acid and oxidizing condition.

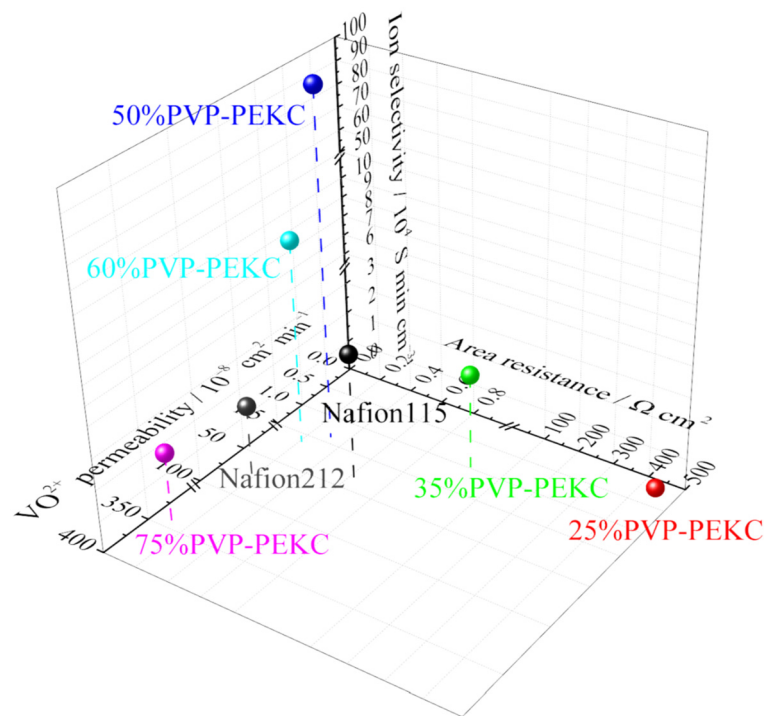


**Figure 8.** Ion selectivity of various membranes after immersing in 3 M  $\text{H}_2\text{SO}_4$  at RT.

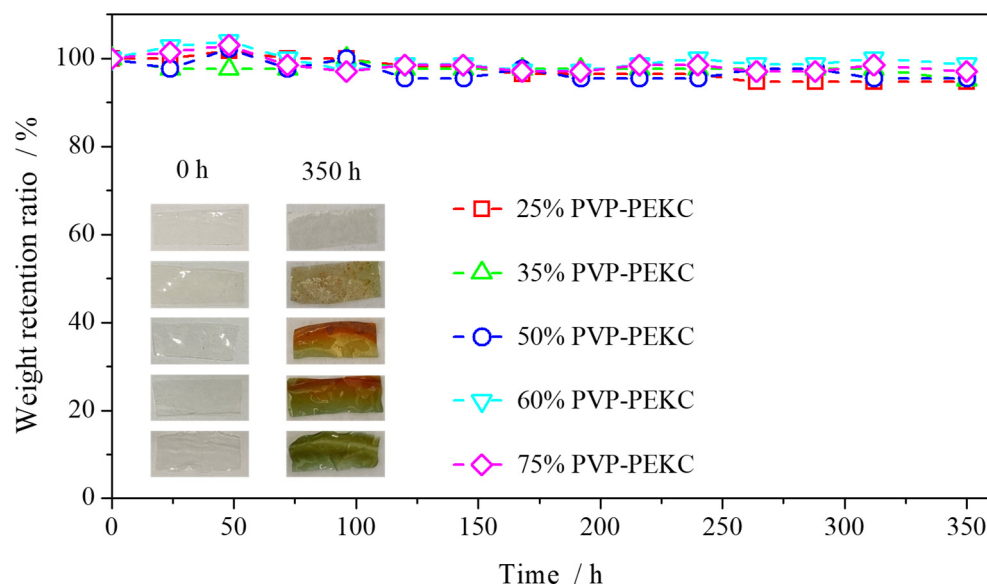


**Figure 9.** Weight retention ratio of  $x\%$ PVP-PEKC membranes during the chemical stability test in 1.5 M  $\text{VO}_2^+$  solution.

### 3.7. VRFB Performance

Comprehensively considering the AR and vanadium ion permeability results, 50%PVP-PEKC and Nafion115 membranes were chosen to assemble VRFBs and investigate their battery performance. Figure 10A shows the characteristic charge–discharge curves of

batteries based on 50%PVP-PEKC and Nafion115 at  $80 \text{ mA cm}^{-2}$ . The cell with 50%PVP-PEKC membrane showed a lower charge voltage and higher discharge voltage than the cell based on Nafion115, due to the lower AR of the 50%PVP-PEKC membrane [9,18]. Moreover, the charge and discharge time of the battery with 50%PVP-PEKC membrane was larger than that of Nafion115, which is due to the lower vanadium ion penetration of the 50%PVP-PEKC membrane [22,55]. Operating a battery at increased current densities is rewarding for higher output power density, reduced galvanic pile size and decreased system manufacture cost [2,4].

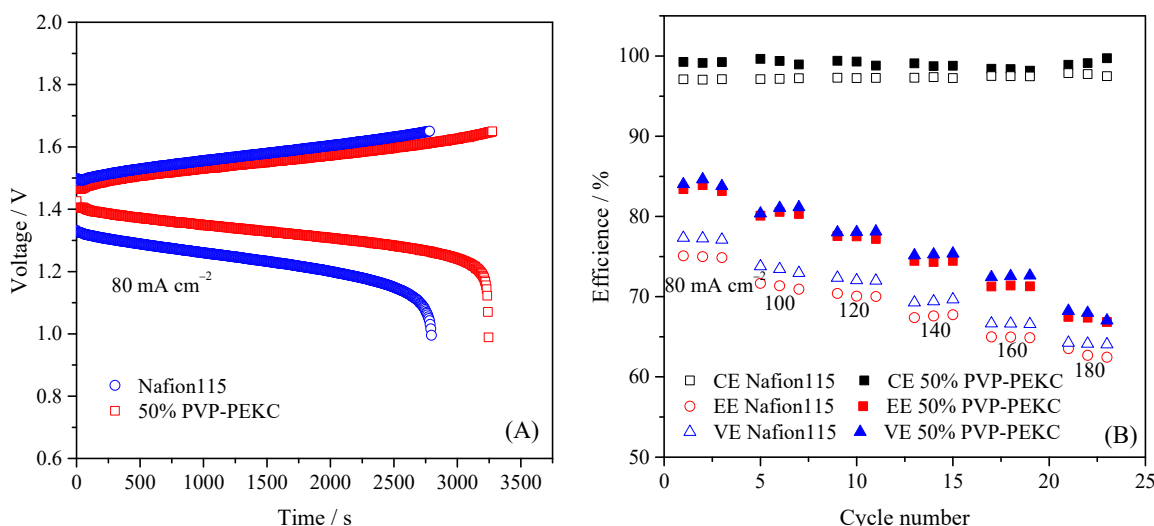


**Figure 10.** (A) Charge–discharge curves of batteries with 50%PVP-PEKC and Nafion115 membranes at  $80 \text{ mA cm}^{-2}$ ; (B) battery performance of CE, VE and EE at different current densities.

Figure 10B depicts the CE, VE and EE of— VRFBs equipped with 50%PVP-PEKC and Nafion115 at  $80\text{--}180 \text{ mA cm}^{-2}$ . The CEs (~99%) of 50%PVP-PEKC membrane were higher than that of Nafion115 (~97%) due to its low vanadium ion permeability. It is not arduous to see that VEs of both cells were declined as increasing the current density, mainly due to the enhanced ohmic polarization of the battery at high current densities, which likewise led to declined EE [10]. Nevertheless, the VEs of VRFB with the 50%PVP-PEKC membrane were higher than those of Nafion115-based cells under all the current densities, distinctly owing to the low AR of the 50%PVP-PEKC membrane. Accordingly, the battery equipped with the 50%PVP-PEKC membrane manifested higher EE than Nafion115 at identical current density. As an example, the EE of 50%PVP-PEKC based cell was 83.8% at  $80 \text{ mA cm}^{-2}$ , while the value of Nafion115 was 77.4%. In addition, Table S1 summarized the comparisons of the battery efficiencies at  $80 \text{ mA cm}^{-2}$  based on different membranes in this work and literature. It can be seen that the 50%PVP-PEKC membrane had comparable or even better cell performances comparing with both PVP blend and other type membranes. For example, the SPEEK/PVP-30%-based cell exhibited an EE% of 84.5% at  $80 \text{ mA cm}^{-2}$  [37], while the cell with the poly [2,2'-(2-benzimidazole-p-phenylene)-5,5'-bibenzimidazole] membrane displayed an EE% of 82% [19]. Moreover, the improved battery performance could be expected by further optimizing the electrode component and operation condition [3–45]. According to these results, it implies that the 50%PVP-PEKC membrane with superior ion selectivity brought about a superior VRFB performance.

Figure 11A presents the cycling performance of the VRFB equipped with 50%PVP-PEKC at  $100 \text{ mA cm}^{-2}$ . Obviously, the 50%PVP-PEKC was stable and maintained almost unchanged CE, VE and EE during the entire cycles. For instance, the EE of the 50%PVP-PEKC based VRFB reduced from 78.1% to 77.6% after 225 cycles, while the EE of the cell with Nafion115 declined from 74.0% to 69.1% after 225 cycles. Above phenomenon is probably due to the incomplete reaction of the active species since none electrolyte rebalance was adopted in the present work [4]. Figure 11B depicts the discharge capacity

retention ratios of the two cells. Owing to the active species imbalance in the electrolyte and the oxygen and hydrogen evolution side reactions at positive and negative electrodes, the capacity of the battery will decline during the long-time test [56,57]. It can be seen from Figure 11B that the capacity decreased trend of the cells equipped with 50%PVP-PEKC and Nafion115 membranes was similar in the first 25 cycles, which may be due to the fact that the Nafion115 membrane has nearly twice of the thickness of the 50%PVP-PEKC membrane, which can prevent ion crossover [58]. In the subsequent cycles, the discharge capacity retention ratio of Nafion115 was about 19%, while the cell equipped with the 50%PVP-PEKC membrane exhibited a much higher discharge capacity retention ratio of around 43% after 225 cycles. This result also proves that the 50%PVP-PEKC membrane occupied lower vanadium ion penetration [19]. In addition, if only considering the cost of raw materials from Sigma, the fabricating cost of the 50%PVP-PEKC blend membrane is as low as \$9–20 m<sup>-2</sup>, comparing with that of the commercial Nafion115 (\$500–700 m<sup>-2</sup>) [59]. Therefore, the x%PVP-PEKC membrane with excellent battery performance would be used as an extremely promising material for VRFBs and other electrochemical energy storage devices [60,61].

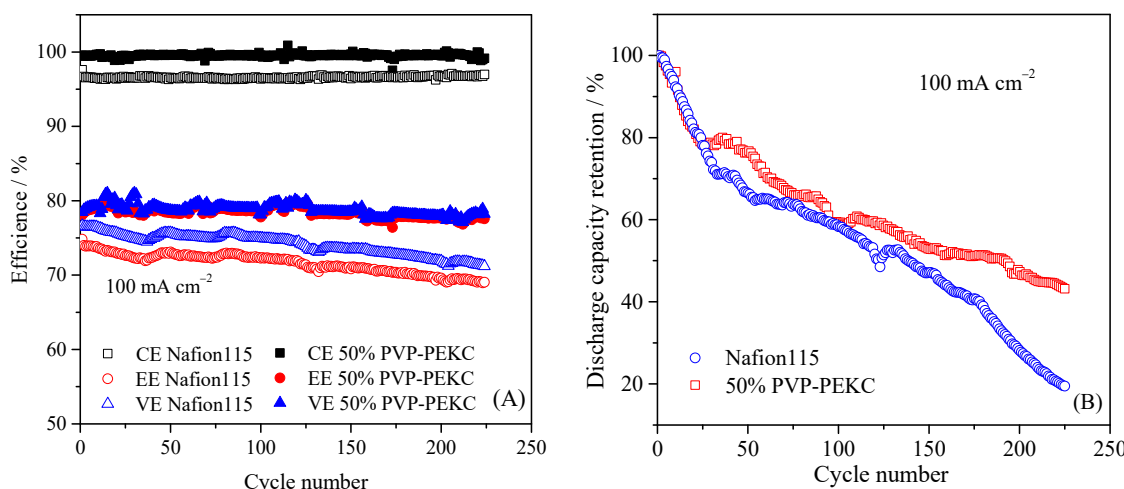


**Figure 11.** (A) Cycling performance of efficiencies of batteries with 50%PVP-PEKC and Nafion115 membranes at 100 mA cm<sup>-2</sup> and (B) discharge capacity retention at 100 mA cm<sup>-2</sup>.

#### 4. Conclusions

Herein, using hydrophilic PVP and rigid PEKC as basic materials, a series of high-performance and low-cost blend membranes for VRFBs were prepared. FT-IR spectra confirmed the successful preparation of the x%PVP-PEKC blend membranes, while SEM results showed a smooth, non-porous and dense structure. Due to the interaction of pyrrolidone and sulfonic acid, x%PVP-PEKC blend membranes exhibited superior SA absorption content and low area resistance. The ADL results indicated that SA molecules were protonated the PVP and in form of “bound acid” in the blend membranes. The protonated PVP polymer chain and hydrophobic PEKC macromolecular network effectively blocked the penetration of vanadium ions. Comprehensively, the ion selectivity of 50%PVP-PEKC membrane was  $103 \times 10^4$  S min cm<sup>-3</sup>, and was closely 17 and 38 times of Nafion115 and Nafion212. The VFRB fixed with 50%PVP-PEKC membrane occupied higher CE (99.3%), VE (84.6%) and EE (83.9%) than Nafion115 (CE: 97.6%, VE: 79.3%, EE: 77.4%) at 80 mA cm<sup>-2</sup>. Simultaneously, the cell with 50%PVP-PEKC exhibited superior cycle stability during charge-discharge cycles at 100 mA cm<sup>-2</sup>. Therefore, x%PVP-PEKC blend membranes possess broad application prospects in the field of VRFBs because of the ascendancy of high efficiencies, knockdown price and simple preparation method.

**Supplementary Materials:** The following supporting information can be downloaded at: <https://www.mdpi.com/article/10.3390/batteries8110230/s1>, Figure S1. Surface SEM images of 25%PVP-PEKC, 50%PVP-PEKC and 75%PVP-PEKC. Table S1: Comparison of the battery performance of various membranes in this work and literature at the current density of  $80 \text{ mA cm}^{-2}$ . Refs. [62–68] are cited in the supplementary materials.

**Author Contributions:** Conceptualization, T.M. and J.Y.; methodology, T.M., S.L. and W.T.; validation, N.S.; formal analysis, W.T.; investigation, N.S. and G.W.; resources, J.Y.; data curation, S.L. and W.T.; writing—original draft preparation, T.M. and J.Y.; writing—review and editing, T.M. and J.Y.; supervision, J.Y.; project administration, J.Y.; funding acquisition, J.Y. All authors have read and agreed to the published version of the manuscript.

**Funding:** This research was funded by Natural Science Foundation of Liaoning Province, grant number 2020-MS-087; and Fundamental Research Funds for the Central Universities of China, grant number N2005026.

**Data Availability Statement:** The data presented in this study are available on request from the corresponding author.

**Acknowledgments:** The authors thank Jianguo Liu of the Chinese Academy of Sciences for the valuable assistance in the vanadium redox flow battery testing.

**Conflicts of Interest:** The authors declare no conflict of interest.

## References

1. Soloveichik, G.L. Flow batteries: Current status and trends. *Chem. Rev.* **2015**, *115*, 11533–11558. [[CrossRef](#)] [[PubMed](#)]
2. López-Vizcaíno, R.; Mena, E.; Millán, M.; Rodrigo, M.A.; Lobato, J. Performance of a vanadium redox flow battery for the storage of electricity produced in photovoltaic solar panels. *Renew. Energy* **2017**, *114*, 1123–1133. [[CrossRef](#)]
3. Minke, C.; Turek, T. Materials, system designs and modelling approaches in techno-economic assessment of all-vanadium redox flow batteries-A review. *J. Power Sources* **2018**, *376*, 66–81. [[CrossRef](#)]
4. Ye, R.J.; Henkensmeier, D.; Yoon, S.J.; Huang, Z.F.; Kim, D.K.; Chang, Z.J.; Kim, S.; Chen, R.Y. Redox flow batteries for energy storage: A technology review. *J. Electrochem. Energy Convers. Storage* **2018**, *15*, 010801. [[CrossRef](#)]
5. Shi, Y.; Eze, C.; Xiong, B.; He, W.; Zhang, H.; Lim, T.; Ukil, A.; Zhao, J. Recent development of membrane for vanadium redox flow battery applications: A review. *Appl. Energy* **2019**, *238*, 202–224. [[CrossRef](#)]
6. Zeng, L.; Zhao, T.S.; Wei, L.; Jiang, H.R.; Wu, M.C. Anion exchange membranes for aqueous acid-based redox flow batteries: Current status and challenges. *Appl. Energy* **2019**, *233*, 622–643. [[CrossRef](#)]
7. Yuan, X.; Song, C.; Platt, A.; Zhao, N.; Wang, H.; Li, H.; Fatih, K.; Jang, D. A review of all-vanadium redox flow battery durability: Degradation mechanisms and mitigation strategies. *Int. J. Energy Res.* **2019**, *43*, 6599–6638. [[CrossRef](#)]
8. Tempelman, C.H.L.; Jacobs, J.F.; Balzer, R.M.; Degirmenci, V. Membranes for all vanadium redox flow batteries. *J. Energy Storage* **2020**, *32*, 101754. [[CrossRef](#)]
9. Austing, J.G.; Kirchner, C.N.; Komsikska, L.; Wittstock, G. Layer-by-layer modification of Nafion membranes for increased life-time and efficiency of vanadium/air redox flow batteries. *J. Membr. Sci.* **2016**, *510*, 259–269. [[CrossRef](#)]
10. Jiang, B.; Wu, L.; Yu, L.; Qiu, X.; Xi, J. A comparative study of Nafion series membranes for vanadium redox flow batteries. *J. Membr. Sci.* **2016**, *510*, 18–26. [[CrossRef](#)]
11. Ye, J.; Yuan, D.; Ding, M.; Long, Y.; Long, T.; Sun, L.; Jia, C. A cost-effective nafion/lignin composite membrane with low vanadium ion permeation for high performance vanadium redox flow battery. *J. Power Sources* **2021**, *482*, 229023. [[CrossRef](#)]
12. Yuan, Z.; Li, X.; Hu, J.; Xu, W.; Cao, J.; Zhang, H. Degradation mechanism of sulfonated poly(ether ether ketone) (SPEEK) ion exchange membranes under vanadium flow battery medium. *Phys. Chem. Chem. Phys.* **2014**, *16*, 19841–19847. [[CrossRef](#)]
13. Sun, C.; Chen, J.; Zhang, H.; Han, X.; Luo, Q. Investigations on transfer of water and vanadium ions across Nafion membrane in an operating vanadium redox flow battery. *J. Power Sources* **2010**, *195*, 890–897. [[CrossRef](#)]
14. Shin, D.W.; Guiver, M.D.; Lee, Y.M. Hydrocarbon-based polymer electrolyte membranes: Importance of morphology on ion transport and membrane stability. *Chem. Rev.* **2017**, *117*, 4759–4805. [[CrossRef](#)] [[PubMed](#)]
15. Zhang, Q.; Dong, Q.-F.; Zheng, M.-S.; Tian, Z.-W. The preparation of a novel anion-exchange membrane and its application in all-vanadium redox batteries. *J. Membr. Sci.* **2012**, *421–422*, 232–237. [[CrossRef](#)]
16. Chen, D.; Hickner, M.A.  $\text{V}^{5+}$  degradation of sulfonated Radel membranes for vanadium redox flow batteries. *Phys. Chem. Chem. Phys.* **2013**, *15*, 11299–11305. [[CrossRef](#)]
17. Glipa, X.; Bonnet, B.; Mula, B.; Jones, D.J.; Rozière, J. Investigation of the conduction properties of phosphoric and sulfuric acid doped polybenzimidazole. *J. Mater. Chem.* **1999**, *9*, 3045–3049. [[CrossRef](#)]
18. Zhou, X.; Zhao, T.; An, L.; Wei, L.; Zhang, C. The use of polybenzimidazole membranes in vanadium redox flow batteries leading to increased coulombic efficiency and cycling performance. *Electrochim. Acta* **2015**, *153*, 492–498. [[CrossRef](#)]

19. Jang, J.K.; Kim, T.H.; Yoon, S.J.; Lee, J.Y.; Lee, J.C.; Hong, Y.T. Highly proton conductive, dense polybenzimidazole membranes with low permeability to vanadium and enhanced H<sub>2</sub>SO<sub>4</sub> absorption capability for use in vanadium redox flow batteries. *J. Mater. Chem. A* **2016**, *4*, 14342–14355. [[CrossRef](#)]
20. Jung, M.; Lee, W.; Noh, C.; Konovalova, A.; Yi, G.S.; Kim, S.; Kwon, Y.; Henkensmeier, D. Blending polybenzimidazole with an anion exchange polymer increases the efficiency of vanadium redox flow batteries. *J. Membr. Sci.* **2019**, *580*, 110–116. [[CrossRef](#)]
21. Hu, L.; Gao, L.; Zhang, C.K.; Yan, X.M.; Jiang, X.B.; Zheng, W.J.; Ruan, X.H.; Wu, X.M.; Yu, G.H.; He, G.H. “Fishnet-like” ion-selective nanochannels in advanced membranes for flow batteries. *J. Mater. Chem. A* **2019**, *7*, 21112–21119. [[CrossRef](#)]
22. Ren, X.R.; Zhao, L.N.; Che, X.F.; Cai, Y.Y.; Li, Y.Q.; Li, H.H.; Chen, H.; He, H.X.; Liu, J.; Yang, J. Quaternary ammonium groups grafted polybenzimidazole membranes for vanadium redox flow battery applications. *J. Power Sources* **2020**, *457*, 228037. [[CrossRef](#)]
23. Shi, M.Q.; Dai, Q.; Li, F.; Li, T.Y.; Hou, G.J.; Zhang, H.M.; Li, X.F. Membranes with well-defined selective layer regulated by controlled solvent diffusion for high power density flow battery. *Adv. Energy Mater.* **2020**, *10*, 2001382. [[CrossRef](#)]
24. Luo Ta David, O.; Gendel, Y.; Wessling, M. Porous poly(benzimidazole) membrane for all vanadium redox flow battery. *J. Power Sources* **2016**, *312*, 45–54.
25. Li, Q.F.; Jensen, J.O.; Savinell, R.F.; Bjerrum, N.J. High temperature proton exchange membranes based on polybenzimidazoles for fuel cells. *Prog. Polym. Sci.* **2009**, *34*, 449–477. [[CrossRef](#)]
26. Zhang, Y.Y.; Xie, Z.C.; Min, X.Q.; Yuan, A.B.; Xu, J.Q. NaCl-templated and polyvinylpyrrolidone-assisted fabrication of a MnO/C-rGO composite as a high-capacity anode material for Li-Ion batteries. *Energy Technol.* **2020**, *8*, 1901194. [[CrossRef](#)]
27. Aili, D.; Kraglund, M.R.; Tavacoli, J.; Chatzichristodoulou, C.; Jensen, J.O. Polysulfone-polyvinylpyrrolidone blend membranes as electrolytes in alkaline water electrolysis. *J. Membr. Sci.* **2020**, *598*, 117674. [[CrossRef](#)]
28. Contardi, M.; Kossyvaki, D.; Picone, P.; Summa, M.; Guo, X.; Heredia-Guerrero, J.A.; Giacomazza, D.; Carzino, R.; Goldoni, L.; Scoponi, G.; et al. Electrospun polyvinylpyrrolidone(PVP) hydrogels containing hydroxycinnamic acid derivatives as potential wound dressings. *Chem. Eng. J.* **2021**, *409*, 128144. [[CrossRef](#)]
29. Del Prado, A.; Civantos, A.; Martinez-Campos, E.; Levkin, P.A.; Reinecke, H.; Gallardo, A.; Elvira, C. Efficient and Low Cytotoxicity Gene Carriers Based on Amine-Functionalized Polyvinylpyrrolidone. *Polymers* **2020**, *12*, 2724. [[CrossRef](#)]
30. Younes, M.; Aquilina, G.; Castle, L.; Engel, K.H.; Fowler, P.; Furst, P.; Gurtler, R.; Gundert-Remy, U.; Husoy, T.; Manco, M.; et al. Re-evaluation of polyvinylpyrrolidone (E 1201) and polyvinylpolypyrrolidone (E 1202) as food additives and extension of use of polyvinylpyrrolidone (E 1201). *EFSA J.* **2020**, *18*, 6215.
31. Bali, M.; Masalci, O. Interactions of cationic surfactants with polyvinylpyrrolidone (PVP): Effects of counter ions and temperature. *J. Mol. Liq.* **2020**, *303*, 112576. [[CrossRef](#)]
32. Mao, T.Y.; Lu, G.; Xu, C.Y.; Yu, H.W.; Yu, J.L. Preparation and properties of polyvinylpyrrolidone-cuprous oxide microcapsule antifouling coating. *Prog. Org. Coat.* **2020**, *141*, 105317. [[CrossRef](#)]
33. Wu, C.X.; Lu, S.F.; Wang, H.N.; Xu, X.; Peng, S.K.; Tan, Q.L.; Xiang, Y. A novel polysulfone-polyvinylpyrrolidone membrane with superior proton-to-vanadium ion selectivity for vanadium redox flow batteries. *J. Mater. Chem. A* **2016**, *4*, 1174–1179. [[CrossRef](#)]
34. Ren, X.R.; Li, H.H.; Liu, K.; Lu, H.Y.; Yang, J.S.; He, R.H. Preparation and investigation of reinforced PVP blend membranes for high temperature polymer electrolyte membranes. *Fiber. Polym.* **2018**, *19*, 2449–2457. [[CrossRef](#)]
35. Guo, Z.B.; Xu, X.; Xiang, Y.; Lu, S.F.; Jiang, S.P. New anhydrous proton exchange membranes for high-temperature fuel cells based on PVDF-PVP blended polymers. *J. Mater. Chem. A* **2015**, *3*, 148–155. [[CrossRef](#)]
36. Zeng, L.; Zhao, T.S.; Wei, L.; Zeng, Y.K.; Zhang, Z.H. Polyvinylpyrrolidone-based semi-interpenetrating polymer networks as highly selective and chemically stable membranes for all vanadium redox flow batteries. *J. Power Sources* **2016**, *327*, 374–383. [[CrossRef](#)]
37. Li, A.F.; Wang, G.; Wei, X.Y.; Li, F.; Zhang, M.M.; Zhang, J.; Chen, J.W.; Wang, R.L. Highly selective sulfonated poly(ether ether ketone)/ polyvinylpyrrolidone hybrid membranes for vanadium redox flow batteries. *J. Mater. Sci.* **2020**, *55*, 16822–16835. [[CrossRef](#)]
38. Chen, F.Y.; Che, X.F.; Ren, X.R.; Zhao, L.N.; Zhang, D.H.; Chen, H.; Liu, J.G.; Yang, J.S. Polybenzimidazole and polyvinylpyrrolidone blend membranes for vanadium flow battery. *J. Electrochem. Soc.* **2020**, *167*, 060511. [[CrossRef](#)]
39. Li, W.; Wang, H.N.; Zhang, J.; Xiang, Y.; Lu, S.F. Advancements of polyvinylpyrrolidone-based polymer electrolyte membranes for electrochemical energy conversion and storage devices. *ChemSusChem* **2022**, *15*, e202200071. [[CrossRef](#)] [[PubMed](#)]
40. Chen, J.H.; Liu, Q.L.; Zhu, A.M.; Fang, J.; Zhang, Q.G. Dehydration of acetic acid using sulfonation cardo polyetherketone (SPEK-C) membranes. *J. Membr. Sci.* **2008**, *308*, 171–179. [[CrossRef](#)]
41. Liu, R.H.; Che, X.F.; Chen, X.; Li, H.; Dong, J.H.; Hao, Z.; Yang, J.S. Preparation and investigation of 1-(3-aminopropyl)imidazole functionalized polyvinyl chloride/poly (ether ketone cardo) membranes for HT-PEMFCs. *Sustain. Energy Fuels* **2020**, *4*, 6066–6074. [[CrossRef](#)]
42. Liu, R.H.; Wang, J.; Che, X.F.; Wang, T.; Aili, D.; Li, Q.F.; Yang, J.S. Facile synthesis and properties of cardo poly(ether ketone)s bearing heterocycle groups for high temperature polymer electrolyte membrane fuel cells. *J. Membr. Sci.* **2021**, *636*, 119584. [[CrossRef](#)]
43. Wang, T.; Jin, Y.P.; Mu, T.; Wang, T.T.; Yang, J.S. Tröger’s base polymer blended with poly(ether ketone cardo) for high temperature proton exchange membrane fuel cell applications. *J. Membr. Sci.* **2022**, *654*, 120539. [[CrossRef](#)]

44. Russell, T.H.; Edwards, B.J.; Khomami, B. Characterization of the Flory-Huggins interaction parameter of polymer thermodynamics. *Europhys. Lett.* **2014**, *108*, 66003. [[CrossRef](#)]
45. Xu, R.S.; Li, L.; Hou, M.J.; Xue, J.J.; Liu, Y.Z.; Pan, Z.L.; Song, C.W.; Wang, T.H. Enhanced CO<sub>2</sub> permeability of thermal crosslinking membrane via sulfonation/desulfonation of phenolphthalein-based cardo poly(arylene ether ketone). *J. Membr. Sci.* **2020**, *598*, 117824. [[CrossRef](#)]
46. Ghimire, P.C.; Bhattacharai, A.; Lim, T.M.; Wai, N.; Skyllas-Kazacos, M.; Yan, Q. In-situ tools used in vanadium redox flow battery research-review. *Batteries* **2021**, *7*, 53. [[CrossRef](#)]
47. Li, X.B.; Ma, H.W.; Wang, P.; Liu, Z.C.; Peng, J.W.; Hu, W.; Jiang, Z.H.; Liu, B.J.; Guiver, M.D. Highly conductive and mechanically stable imidazole-rich cross-linked networks for high-temperature proton exchange membrane fuel cells. *Chem. Mater.* **2020**, *32*, 1182–1191. [[CrossRef](#)]
48. Noh, C.; Jung, M.; Henkensmeier, D.; Nam, S.W.; Kwon, Y.C. Vanadium redox flow batteries using meta-polybenzimidazole-based membranes of different thicknesses. *ACS Appl. Mater. Interfaces* **2017**, *9*, 36799–36809. [[CrossRef](#)]
49. Tianjin University. *Physical Chemistry*; High Education Press: Beijing, China, 2017.
50. Lou, X.C.; Lu, B.; He, M.R.; Yu, Y.S.; Zhu, X.B.; Peng, F.; Qin, C.P.; Ding, M.; Jia, C.K. Functionalized carbon black modified sulfonated polyether ether ketone membrane for highly stable vanadium redox flow battery. *J. Membr. Sci.* **2022**, *643*, 120015. [[CrossRef](#)]
51. Park, D.-J.; Jeon, K.-S.; Ryu, C.-H.; Hwang, G.-J. Performance of the all-vanadium redox flow battery stack. *J. Ind. Eng. Chem.* **2017**, *45*, 387–390. [[CrossRef](#)]
52. Ahn, Y.; Kim, D. Anion exchange membrane prepared from imidazolium grafted poly (arylene ether ketone) with enhanced durability for vanadium redox flow battery. *J. Ind. Eng. Chem.* **2019**, *71*, 361–368. [[CrossRef](#)]
53. Chae, I.; Luo, T.; Moon, G.H.; Ogieglo, W.; Kang, Y.S.; Wessling, M. Ultra-High proton/vanadium selectivity for hydrophobic polymer membranes with intrinsic nanopores for redox flow battery. *Adv. Energy Mater.* **2016**, *6*, 1600517. [[CrossRef](#)]
54. Jiang, H.R.; Sun, J.; Wei, L.; Wu, M.C.; Shyy, W.; Zhao, T.S. A high power density and long cycle life vanadium redox flow battery. *Energy Storage Mater.* **2020**, *24*, 529–540. [[CrossRef](#)]
55. Zhang, B.; Wang, Q.; Guan, S.; Weng, Z.; Zhang, E.; Wang, G.; Zhang, Z.; Hu, J.; Zhang, S. High performance membranes based on new 2-adamantane containing poly(aryl ether ketone) for vanadium redox flow battery applications. *J. Power Sources* **2018**, *399*, 18–25. [[CrossRef](#)]
56. Jiang, B.; Yu, L.H.; Wu, L.T.; Mu, D.; Liu, L.; Xi, J.Y.; Qiu, X.P. Insights into the impact of the Nafion membrane pretreatment process on vanadium flow battery performance. *ACS Appl. Mater. Interfaces* **2016**, *8*, 12228–12238. [[CrossRef](#)]
57. Yu, L.H.; Lin, F.; Xiao, W.D.; Xu, L.; Xi, J.Y. Achieving efficient and inexpensive vanadium flow battery by combining Ce<sub>x</sub>Zr<sub>1-x</sub>O<sub>2</sub> electrocatalyst and hydrocarbon membrane. *Chem. Eng. J.* **2019**, *356*, 622–631. [[CrossRef](#)]
58. Xing, Y.; Geng, K.; Chu, X.M.; Wang, C.Y.; Liu, L.; Li, N.W. Chemically stable anion exchange membranes based on C<sub>2</sub>-protected imidazolium cations for vanadium flow battery. *J. Membr. Sci.* **2021**, *618*, 118696. [[CrossRef](#)]
59. Yuan, Z.Z.; Duan, Y.Q.; Zhang, H.Z.; Li, X.F.; Zhang, H.M.; Vankelecom, I. Advanced porous membranes with ultra-high selectivity and stability for vanadium flow batteries. *Energy Environ. Sci.* **2016**, *9*, 441–447. [[CrossRef](#)]
60. Zhang, B.K.; Yang, L.Y.; Li, S.N.; Pan, F. Progress of lithium-ion transport mechanism in solid-state electrolytes. *J. Electrochem.* **2021**, *27*, 269–277.
61. Chen, J.J.; Dong, Q.F. Research progress of key components in lithium-sulfur batteries. *J. Electrochem.* **2020**, *26*, 648–662.
62. Che, X.F.; Zhao, H.; Ren, X.R.; Zhang, D.H.; Wei, H.; Liu, J.G.; Zhang, X.; Yang, J.S. Porous polybenzimidazole membranes with high ion selectivity for the vanadium redox flow battery. *J. Membr. Sci.* **2020**, *611*, 118359. [[CrossRef](#)]
63. Teng, X.G.; Dai, J.C.; Su, J.; Zhu, Y.M.; Liu, H.P.; Song, Z.J. A high performance polytetrafluoroethylene/Nafion composite membrane for vanadium redox flow battery application. *J. Power Sources* **2013**, *240*, 131–139. [[CrossRef](#)]
64. Dai, X.J.; Yu, L.H.; Li, Z.H.; Yan, J.; Liu, L.; Xi, J.Y.; Qiu, X.P. Sulfonated Poly(Ether Ether Ketone)/Graphene composite membrane for vanadium redox flow battery. *Electrochim. Acta* **2014**, *132*, 200–207. [[CrossRef](#)]
65. Tang, W.Q.; Yang, Y.F.; Liu, X.L.; Dong, J.H.; Li, H.H.; Yang, J.S. Long side-chain quaternary ammonium group functionalized polybenzimidazole based anion exchange membranes and their applications. *Electrochim. Acta* **2021**, *391*, 138919. [[CrossRef](#)]
66. Lu, W.J.; Shi, D.Q.; Zhang, H.M.; Li, X.F. Advanced poly(vinyl pyrrolidone) decorated chlorinated polyvinyl chloride membrane with low area resistance for vanadium flow battery. *J. Membr. Sci.* **2021**, *620*, 118947. [[CrossRef](#)]
67. Li, Y.; Zhang, H.M.; Li, X.F.; Zhang, H.Z.; Wei, W.P. Porous poly (ether sulfone) membranes with tunable morphology: Fabrication and their application for vanadium flow battery. *J. Power Sources* **2013**, *233*, 202–208. [[CrossRef](#)]
68. Tang, W.Q.; Mu, T.; Che, X.F.; Dong, J.H.; Yang, J.S. Highly selective anion exchange membrane based on quaternized poly(triphenyl piperidine) for the vanadium redox flow battery. *ACS Sustain. Chem. Eng.* **2021**, *9*, 14297–14306. [[CrossRef](#)]